Using Thorium Based Fuel in AP1000: Steady State Analysis

H. K. Selim[1], E. H. Amin[1], H. E. Roushdy[2]
(1) Department of Nuclear Safety Engineering, Nuclear and Radiological Regulatory Authority, Cairo, Egypt
(2) Engineering Physics Department, Faculty of Engineering, Cairo University, Giza, Egypt

The feasibility of utilizing Thorium-Plutonium Mixed Oxide in the Westinghouse AP1000 Advanced Passive pressurized water reactor is examined under steady-state, beginning of life (BOL) conditions. Initial core loading of the reactor consists of three types of UO_2 fuel assemblies with different enrichment in U235, as follows: 2.35w/o, 3.40w/o and 4.45w/o. In this paper, one-third of the UO_2 fuel assemblies are replaced by $(Th-Pu)O_2$ fuel assemblies in two arrangements: the first one assumes a blanket of $(Th-Pu)O_2$ fuel which replaces the 4.45% enriched UO_2 fuel assemblies surrounding the low enriched UO_2 fuel assemblies, and in the second arrangement some of the UO_2 fuel assemblies are replaced in a way creating a ring of $(Th-Pu)O_2$ fuel in the core. The reactor is modeled using QUARK computer code. The required cross-section data for QUARK calculations have been generated using WIMSD5 lattice cell code. The results of the steady state analysis show that introducing $(Th-Pu)O_2$ fuel into AP1000 would not negatively impact the reactor's safety as the criteria mentioned in design control document are met. For $(Th-Pu)O_2$ fuel blanket and ring loading arrangements, the calculated power peaking factor is less or equal to the design limit. Over the length of the hot channel, the Minimum Departure from Nucleate Boiling Ratio (MDNBR) varies with a minimum above the design limit for the considered $(Th-Pu)O_2$ fuel assemblies loading arrangements. This work provides the basis for studying Th-based fuel behavior and thermal hydraulic analysis of AP1000 using Th-based fuel in order to evaluate the safety aspect of various core loading patterns under anticipated and accidental conditions.

Keywords: AP1000; Reactor Safety; Steady-State Analysis; $(Th-Pu)O_2$ fuel; Neutronic/Thermal-Hydraulic Coupling; QUARK; WIMSD5

Introduction

Due to the scarcity of natural uranium resources and a mismatch between the uranium production and the requirements for reactors operation, thorium has been explored as an alternative nuclear fuel to be used in thermal reactors. Past decades of extensive operation of Light Water Reactors (LWRs) have created significant amounts of plutonium, which could be either utilized in future fast reactor systems or stored in final repository. Current practice of Pu recycling in the existing LWRs in the form of U–Pu mixed oxide fuel (MOX) is not efficient due to continuous Pu production from U-238. Consequently, other methods have been proposed to reduce the

plutonium stockpile, such as mixing plutonium with thorium or other inert materials. The use of Th–Pu mixed oxide fuel will considerably improve Pu consumption rates because no new Pu is generated from Th [1, 2]. Th–Pu mixed oxide fuel is anticipated to have a more favorable in-core behavior as compared to MOX fuel, due to its better material properties, including a higher thermal conductivity, a significantly higher melting point, a lower thermal expansion coefficient, and a lower fission-gas release [3].

Preliminary calculations have been carried out by *Klara Insulander Bjork* [4] to investigate the possibility of extending operating cycle length in

PWRs using of Th-Pu mixed oxide fuel. The calculations have been carried out in two dimensions, utilizing the fuel assembly burnup simulation program CASMO-5. The reload scheme and the operating parameters are modeled on the Swedish PWR Ringhals 3, and a normal UOX fuel assembly designed for this reactor has been used as a reference. Results have shown that an extension of the currently employed 12-month operating cycle length is possible, either through using a burnable absorber or with a modified fuel assembly design, assuming the same 3-batch reload scheme as the one currently used in Ringhals 3 PWR. The initial k_{inf} of the new (Th-Pu) mixed oxide fuel project was designed not to exceed the k_{inf} value corresponding to the reference UOX fuel. The calculated power peaking factor is much lower than the reference ones value, but slightly increases with the burn up of the fuel assembly. The calculated values for all reactivity coefficients were within acceptable range. The worth of control rods and soluble boron are lower than the reference, as expected for a plutonium-bearing fuel. *CheukWah Lau et al.* [5] studied the safety aspects of introducing (Th-Pu) mixed oxide fuel in PWRs for two different cases, namely: a full (Th-Pu) mixed oxide core, and a reactor core containing 1/3 (Th-Pu) mixed oxide fuel in combination with the ordinary UOX fuel. It has been shown that the basic safety limits are contained in both cases, but the lower amount of Pu loaded in the 1/3 (Th-Pu) mixed oxide core compared with a full (Th-Pu) mixed oxide core will result in a lower consumption rate of plutonium. However, the lower requirements of control rods and enriched boron, higher fraction of delayed neutrons, reactivity feedback more similar to that of a UOX core, and higher plutonium incineration compared with 30% UOX/MOX core make the implementation of the 1/3 (Th-Pu) mixed oxide core more attractive for initiating plutonium incineration in currently operating commercial LWRs. Additionally, the damping of axial xenon oscillations is more effective for the 1/3 (Th-Pu) mixed oxide core compared with the standard core. The strategy of using 1/3 (Th-Pu) mixed oxide leads to a cheaper and easier way to start using (Th-Pu) mixed oxide fuel assemblies in the near future for reducing the plutonium stockpile. *Naymushin et al.* [6] explored the possibilities of using alternative thorium-based fuel compositions in VVER-type reactors. This study presents a comparison between standard uranium dioxide fuel and perspective fuel composition: thorium dioxide, mixed thorium and plutonium dioxides. The calculation results have shown that using of perspective fuel composition lead to improving reactor core physical and economical characteristics. Furthermore, the investigated fuel provides effective burnup that increases the fuel cycle length.

Safety performance of the reactor at steady state represents the basis for the analysis of the reactor under transient. Fuel characterization under normal operating conditions (steady state conditions) is fundamental, as input data, for studying the fuel behavior under anticipated and accidental conditions [7]. The increased importance of detailed reactor core and fuel assembly description for LWRs, as well as the sub-channel safety analysis, requires coupled neutronic/thermal-hydraulic codes. *Omid Noori-Kalkhoran et al.* [8] analyzed VVER-1000 nuclear reactor core by using the neutronic/thermal hydraulic coupling calculations approach. This calculation approach is based on PARCS v2.7, COBRA-EN and WIMSD-5B computer codes. First, WIMSD-5B lattice cell code has been used to calculate macroscopic cross-sections for each fuel assembly. Neutronic parameters of interest have been calculated by means of PARCS v2.7 code. COBRA-EN was used for thermal-hydraulic parameters calculations for all the fuel assemblies. The proposed coupling can be applied for both steady-state and transient calculations. Neutronic accidents such as REA (Rod Ejection Accident) and thermal-hydraulic accidents such as LOFA (Loss of Flow Accident) can be analyzed by the proposed coupling. In the above mentioned study, steady-state calculations and LOFA have been simulated. The results have been compared to Bushehr Nuclear Power Plant (Iran) Final Safety Analysis Report - FSAR. The results are very similar to those included in FSAR, and confirm the ability of this package to simulate an accident in the reactor core, especially, a thermal-hydraulic accident that is out of the capability of PARCS code, used individually.

Description of the Reactor
AP1000 is an advanced passive pressurized water reactor designed to produce 1117 MWe (~3400 MWth). AP1000 core is composed of 157 fuel assemblies. Each assembly consists of 264 fuel

rods, 24 control rod guide tubes and one central instrumentation guide tube, arranged in a 17x 17 square array. AP1000 core design uses discrete burnable absorbers (PYREX) and integral fuel burnable absorbers (IFBA). PYREX rod is made of borosilicate glass, whereas IFBA rod is a fuel rod with thin boride coating on the fuel. These rods are arranged in different patterns within a fuel assembly and their function is to partly control the core excess reactivity, to limit power peaking factors and to keep the moderator temperature coefficient (MTC) negative at normal operation [9,10].

In order to control relatively rapid reactivity changes and axial power distribution, rod cluster control assemblies (RCCA) are used. AP1000 core contains 69 RCCA, each of these assemblies is consisted of 24 absorber rods. Two types of control rod cluster assemblies are used, i.e. black and gray. Absorber material of black rod is an alloy of Ag-In-Cd in stainless steel clad. The gray rod cluster assembly is similar to the black rod cluster control assembly except that 12 of the 24 rods are fabricated of stainless steel, while the remaining 12 rods are Ag-InCd (of a reduced diameter as compared to the one of RCCA absorber) with stainless steel clad. The gray rod cluster assemblies are used in load follow maneuvers and are named 'Mechanical Shim (MSHIM)', as their operation minimizes the need for changes to the concentration of soluble boron [9,10]. AP1000 design parameters are given in Table(1).

Table (1): AP1000 Design Parameters

Parameters	Value
Reactor core heat output	3400 MW_{th}
System pressure, nominal	2250 psia
System pressure, minimum steady state	2190 psia
Average inlet mass flux	12.45x10^6 kg/hr-m^2
Coolant nominal inlet temperature	552.594 K
Coolant average temperature in core	576.539 K
Average linear power	18.77 kW/m
Core diameter, equivalent	304.04 cm
Core height, cold, active fuel	426.72 cm

Initial core loading

AP1000 initial core loading configuration, obtained from AP1000 Designed Control Documents (DCD)[9], is consisted by three types of UO$_2$ fuel assemblies, with different enrichments

in U^{235}, namely: 2.35w/o, 3.40w/o and 4.45w/o. The highest enriched fuel assemblies are loaded at the core periphery, the other two lower enriched fuel assemblies being arranged in a checkboard pattern in the central portion of core. IFBA rods are distributed in a symmetrical pattern to reduce the pin to pin power peaking. PYREX rods are removable burnable absorbers. Fig.(1) presents the core configuration with fuel, PYREX and IFBA rods. Initial core parameters are given in Table (2).

Modeling Methodology

In this study, calculations were performed using QUARK, (QUAndry based Reactor Kinetics) computer code. QUARK is a combined computer program including a revised version of the QUANDARY three-dimensional, two-group neutron kinetics code and an upgraded version of the COBRA transient core analysis code (COBRA-EN) [11]. The required cross-section data for QUARK have been generated using WIMSD5 code. WIMS (Winfrith Improved Multigroup Scheme) is a multigroup transport code for reactor lattice calculations, including burnup. WIMS has been extensively used throughout the world for power and research reactors lattice analysis [12]. A zero burnup with no Xenon and Samarium effects is assumed everywhere (i.e., B.O.L condition) and the node-dependent burnup weighted coolant densities are set equal to the correspondent instantaneous coolant densities, as soon as they are computed by the thermal-hydraulic model (COBRA-EN model).

A steady state calculation is performed in subcooled conditions (possible subcooled voids have been neglected by selecting the homogeneous model for the steam fraction), the computed Boron concentration was expected to be uniform throughout the core. A single Boron concentration is given in the input and used everywhere to update the nodal cross-sections.

Reactor core modeling

In this paper, in addition to AP1000 initial core loading, alternative core loadings are proposed, assuming that one-third of the UO$_2$ fuel assemblies are replaced by (Th-Pu)O$_2$ fuel assemblies in two arrangements. In first arrangement, a blanket of (Th-Pu)O$_2$ fuel assemblies replaces the 4.45% enriched UO$_2$ fuel assemblies (placed at the core periphery) and surrounds the low enriched UO$_2$. In

the second arrangement, some of the UO_2 fuel assemblies are replaced creating a ring of (Th-Pu)O_2 fuel assemblies in the core. The core configurations used in the proposed analysis are shown in Fig. (2) and the material compositions of (Th-Pu)O_2 fuel are as follows:

Material compositions (atoms/barn.cm): 5% PuO_2 + 95% ThO_2

Th-232	2.0592E-2;
Pu-238	2.2900E-5;
Pu-239	7.4780E-4;
Pu-240	2.9030E-4;
Pu-241	1.5340E-4;
Pu-242	5.0100E-5;
O-16	4.3710E-2

The three core loading schemes were modeled using QUARK code capabilities; radially, the core is divided into cells of 21.4 cm width, each corresponding to one fuel assembly, plus a radial reflector cell of the same width. Axially, the reactor core is divided into 23 layers; the top and bottom layers (reflector) have a thickness of 25.4 cm and the inner 21 layers have a thickness of 20.32 cm each. Each node of the reactor geometry is associated to one of the defined compositions. A complete set of macroscopic cross-sections for transport, scattering, absorption and fission is defined for each composition. Table (3) shows the 2-group macroscopic cross-section for each composition considered for the fuel assemblies in the core.

Fig.1: AP1000 Initial Core Loading

Table (2): AP1000 Core Parameters

Fuel assemblies	
Number	157
Rod array	17X17
Rods per assembly	264
Rod pitch (cm)	1.26
Fuel rods	
Number	41,448
Outside diameter (cm)	0.95
Diameter gap (cm)	0.0165
Clad thickness (cm)	0.0572
Clad material	ZIRLO
Fuel pellets diameter (cm)	0.8191
Rod cluster control assemblies	
Absorber material	Ag-In-Cd
Diameter (cm)	0.866
Cladding material	304SS
Clad thickness (cm)	0.047
Number of clusters	53
Absorber rods per cluster	24
Gray rod cluster control assemblies	
Absorber material	Ag-In-Cd / 304SS
Diameter (cm)	0.406
Cladding material	304SS
Clad thickness (cm)	0.047
Number of clusters	16
Absorber rods per cluster	12 Ag-In-Cd / 12 304SS
Discrete burnable absorber rods (PYREX)	
Material	Borosilicate Glass
Outer diameter (cm)	0.968
Inner tube, Outer diameter (cm)	0.461
Clad and inner tube material	Stainless Steel
B_{10} content (Mg/cm)	6.24
Absorber length (cm)	145
Integrated fuel burnable absorber (IFBA)	
Material	Boride Coating
B_{10} content (Mg/cm)	0.772
Absorber length (cm)	152

(a) 100% UO_2 (b) UO_2/(Th-Pu)O_2 - blanket (c) UO_2/(Th-Pu)O_2 - ring

☐ 2.35% enriched UO_2 ■ 3.40% enriched UO_2 ■ 4.45% enriched UO_2 ☐ UO_2/(Th-Pu)O_2 ■ Reflector
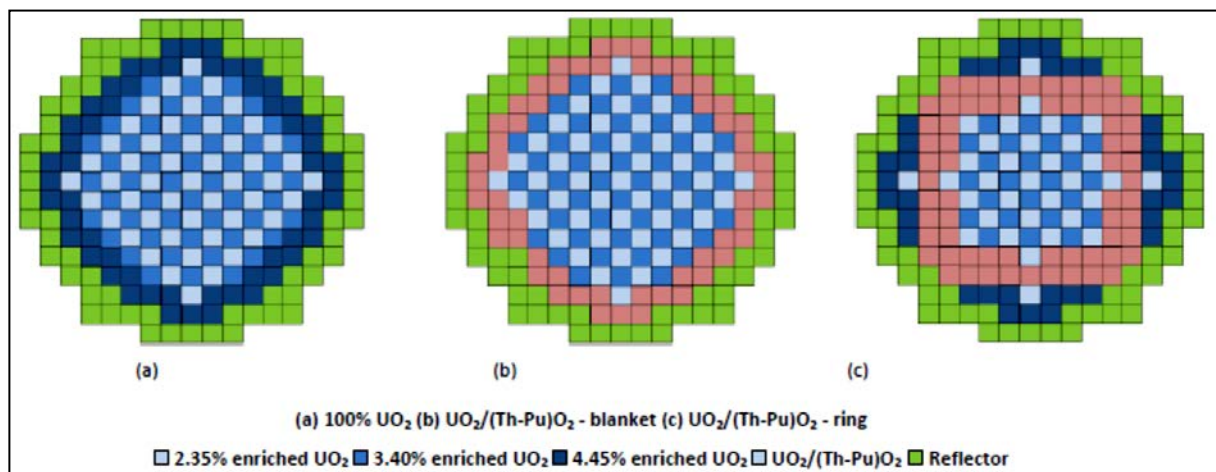
Fig.(2): Core Loading Patterns

Table (3-a): Macroscopic Cross -section – UO$_2$ Fuel Initial Compositions

Composition	Group	$\sum_{tr}$	$\sum_r$	$\sum_f$	$\sum_{21}$
UO$_2$ 2.35 w/o	Fast	0.25802	0.02891	0.00264	0.01918
	Thermal	1.00140	0.07814	0.05200	
UO$_2$ 3.40 w/o, 88 IFBA, 24 BA	Fast	0.25750	0.02911	0.00327	0.01811
	Thermal	1.00061	0.14153	0.06826	
UO$_2$ 3.40 w/o, 28 IFBA, 24 BA	Fast	0.25749	0.02908	0.00328	0.01832
	Thermal	0.99954	0.13309	0.06976	
UO$_2$ 4.45 w/o, 88 IFBA, 12 BA	Fast	0.25713	0.02929	0.00389	0.01762
	Thermal	1.00322	0.14440	0.08461	
UO$_2$ 4.45 w/o, 72 IFBA, 24 BA	Fast	0.25712	0.02922	0.00389	0.01762
	Thermal	1.00268	0.15511	0.08506	
UO$_2$ 4.45 w/o, 88 IFBA, 9 BA	Fast	0.25713	0.02931	0.00389	0.01764
	Thermal	1.00322	0.14101	0.08461	
UO$_2$ 4.45 w/o, 112 IFBA	Fast	0.25713	0.02937	0.00388	0.01760
	Thermal	1.00402	0.13388	0.08393	
UO$_2$ 3.40 w/o, 44 IFBA, 24 BA	Fast	0.25749	0.02909	0.00328	0.01827
	Thermal	0.99983	0.13534	0.06936	
UO$_2$ 2.35 w/o, 28 IFBA	Fast	0.25802	0.02893	0.00263	0.01907
	Thermal	1.00127	0.08272	0.05143	

Table (3-b): Macroscopic Cross-section – (Th-Pu)O$_2$ Fuel Blanket Compositions

Composition	Group	$\sum_{tr}$	$\sum_r$	$\sum_f$	$\sum_{21}$
(Th-Pu)O$_2$, 88 IFBA, 12 BA	Fast	0.25394	0.02850	0.00363	0.01551
	Thermal	1.16533	0.28246	0.16522	
(Th-Pu)O$_2$, 72 IFBA, 24 BA	Fast	0.25393	0.02837	0.00363	0.01551
	Thermal	1.16419	0.28631	0.16558	
(Th-Pu)O$_2$, 88 IFBA, 9 BA	Fast	0.25394	0.02854	0.00363	0.01552
	Thermal	1.16533	0.28091	0.16522	
(Th-Pu)O$_2$, 112 IFBA	Fast	0.25394	0.02865	0.00363	0.01549
	Thermal	1.16703	0.27934	0.16469	

Table (3-c): Macroscopic Cross-section – (Th-Pu)O$_2$ Fuel Ring Compositions

Composition	Group	$\sum_{tr}$	$\sum_r$	$\sum_f$	$\sum_{21}$
(Th-Pu)O$_2$	Fast	0.20211	0.02614	0.00204	0.01770
	Thermal	1.02230	0.15718	0.09865	
(Th-Pu)O$_2$, 88 IFBA, 24 BA	Fast	0.25394	0.02838	0.00363	0.01547
	Thermal	1.16533	0.28831	0.16522	
(Th-Pu)O$_2$, 28 IFBA, 24 BA	Fast	0.25392	0.02835	0.00364	0.01562
	Thermal	1.16109	0.28081	0.16655	
(Th-Pu)O$_2$, 112 IFBA	Fast	0.25394	0.02865	0.00363	0.01549
	Thermal	1.16703	0.27934	0.16469	
(Th-Pu)O$_2$, 44 IFBA, 24 BA	Fast	0.25393	0.02836	0.00364	0.01558
	Thermal	1.16222	0.28281	0.16620	
(Th-Pu)O$_2$, 28 IFBA	Fast	0.25392	0.02861	0.00364	0.01571
	Thermal	1.16109	0.26789	0.16655	

Feedback model

A feedback model is an analytical approximation for the dependence of any macroscopic cross-section (including discontinuity factors) upon the thermal-hydraulic variables. The coefficient-based feedback model, involving fuel temperature, coolant temperature is defined as:

$$\Sigma = \Sigma^* + \frac{\partial \Sigma}{\partial T_f} \left(T_f - T_f^* \right) + \frac{\partial \Sigma}{\partial T_c} \left(T_c - T_c^* \right)$$

where Σ represents any of the following group-dependent macroscopic nuclear parameters:

- diffusion coefficient (D) or transport cross-section (Σ_{tr}),
- capture cross-section (Σ_c),
- scattering removal cross-section (Σ_r),
- neutron production (nufission) cross-section ($\nu\Sigma_f$),
- fission cross-section (Σ_f),

Σ^*, T_f^*, T_c^* are reference values.

The feedback coupling between neutronics and thermal-hydraulic is characterized by the definition of channel region. In the present work, each fuel assembly is defined as channel region. The channel map for 1/8 core (26 channels) is shown in Fig.(3). The channels are classified into three types, namely: whole channels, half channels and half quarter channels (at the center of the core). The channels which are split vertically and those which are split diagonally are considered to be similar since the flow area, wetted and heated perimeter, and the number of heated rods are the same for both. The types of channels and fuels for the three core loading patterns are presented in Table (4).
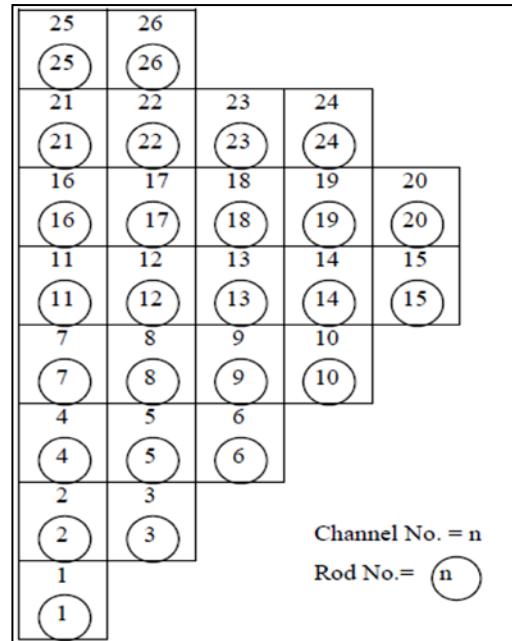

Fig. (3): Channel Map

Table (4): Channels and fuel Types

Loading Pattern	Channel	Fuel Type	Channel Numbers
UO$_2$	whole channel	UO$_2$	5,8,9,12,13,14,17,18,19,20,22,23,24,26
	half channel	UO$_2$	2,3,4,6,7,10,11,15,16,21,25
	half quarter channel	UO$_2$	1
UO$_2$/(Th-Pu)O$_2$ (Blanket)	whole channel	UO$_2$	5,8,9,12,13,14,17,18
	whole channel	(Th-Pu)O$_2$	19,20,22,23,24,26
	half channel	UO$_2$	2,3,4,6,7,10,11,15,16,21
	half channel	(Th-Pu)O$_2$	25
	half quarter cannel	UO$_2$	1
UO$_2$/(Th-Pu)O$_2$ (Ring)	whole channel	UO$_2$	5,8,9,22,23,24,25,26
	whole channel	(Th-Pu)O$_2$	12,13,14,17,18,19,20
	half channel	UO$_2$	2,3,4,6,7,10,11,21
	half channel	(Th-Pu)O$_2$	15,16
	half quarter channel	UO$_2$	1

Results and Discussion

The results obtained for the steady state analysis are summarized in table (5). Normalized assembly averaged power density for 1/8 core was calculated for the three loading patterns using QUARK code, and can be seen in Fig.(4). This parameter calculated values were compared with those from the DCD [9]. The maximum difference obtained is statistically insignificant, as can be noticed in the following: 0.011 for UO$_2$ loading pattern, and 0.059 and 0.014 for the UO$_2$/(Th-Pu)O$_2$ blanket and UO$_2$/(Th-Pu)O$_2$ ring loading patterns,

respectively. Fig. (5) presents the axial normalized peak power density with the peak at nodes (5,1,12), (1,1,12), (1,6,12) for UO$_2$, UO$_2$/(Th-Pu)O$_2$ blanket and UO$_2$/(Th-Pu)O$_2$ ring core loading patterns, respectively. Fig. (6) shows the radial thermal flux distribution for 1/8 core corresponding to the considered loading patterns.

Table(5): Summary Results for Steady State Calculation

Parameter	UO_2	$UO_2/(Th-Pu)O_2$ (Blanket)	$UO_2/(Th-Pu)O_2$ (Ring)
Average total nodal flux ($n/cm^2.s$)	2.095E+14	2.122E+14	2.075E+14
Mean power density (MW/cm^3)	110.819	110.819	110.819
Mean pressure drop (kPa)	98.573	99.926	98.817
Mean hydrostatic head (kPa)	29.642	29.411	29.642
Average fuel temperature (K)	846.97	842.47	834.13
Maximum fuel temperature (K)	1095.41	1290.27	1190.09
Average doppler temperature (K)	714.51	711.73	707.05
Maximum doppler temperature (K)	845.30	949.03	896.23
Maximum fuel enthalpy (MJ/kg) - (cal/g)	0.233 -- 55.784	0.296 - 70.703	0.264 - 63.007
Average coolant temperature (K)	579.18	578.87	578.84
Average coolant density (g/cm3)	0.7083	0.7028	0.7074
Average exit coolant temperature (K)	601.78	600.32	600.86
Average exit coolant density (g/cm3)	0.6485	0.6209	0.6416
Average linear heat rate per fuel rod (kW/m)	19.223	19.223	18.746
Maximum axial hot channel factor	1.497	1.496	1.492
Maximum radial hot channel factor	1.270	1.730	1.720
Power Peaking Factor	1.901	2.588	2.566

UO_2 - Ref.
UO_2
$UO_2/(Th-Pu)O_2$ - Blanket
$UO_2/(Th-Pu)O_2$ - Ring

0.541	0.439			
0.536	0.435			
0.566	0.459			
0.535	0.434			
0.957	0.913	0.815	0.561	
0.949	0.905	0.808	0.556	
1.001	0.955	0.852	0.587	
0.946	0.903	0.806	0.555	
1.161	1.168	1.026	1.041	0.630
1.151	1.158	1.017	1.032	0.625
1.214	1.221	1.073	1.089	0.659
1.148	1.155	1.015	1.029	0.623
1.254	1.113	1.203	1.033	0.859
1.243	1.104	1.193	1.024	0.852
1.311	1.164	1.258	1.080	0.898
1.240	1.101	1.190	1.022	0.850
1.130	1.250	1.111	1.193	
1.120	1.239	1.102	1.183	
1.182	1.307	1.162	1.248	
1.118	1.236	1.099	1.180	
1.268	1.142	1.250		
1.257	1.132	1.239		
1.326	1.194	1.307		
1.254	1.129	1.236		
1.154	1.273			
1.144	1.262			
1.207	1.331			
1.141	1.259			
1.279				
1.268				
1.338				
1.265				

Fig. (4): Normalized Assembly-Averaged Power Density for 1/8 Core
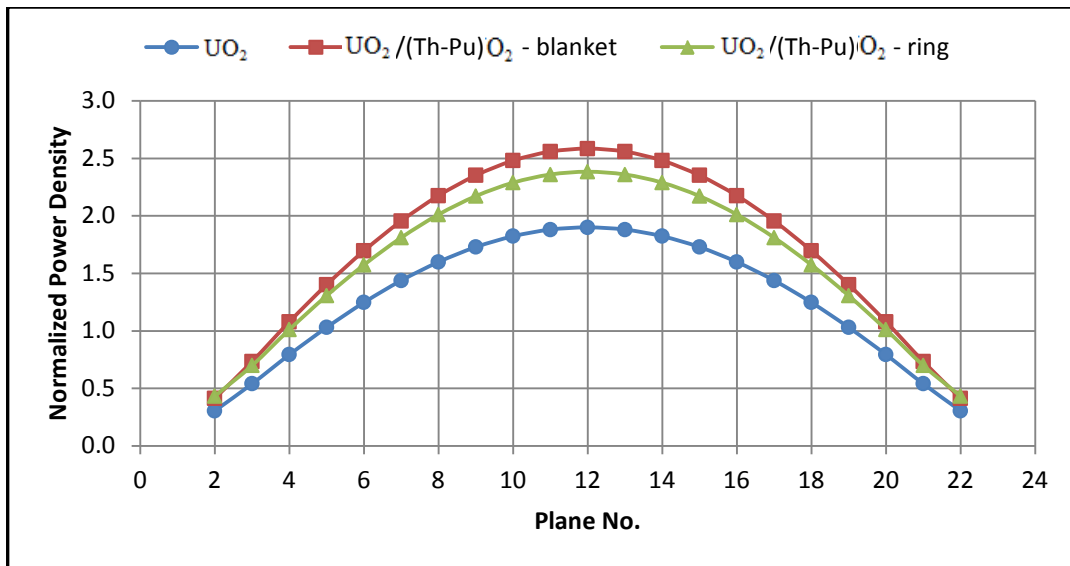
Fig. (5): Axial Normalized Peak Power Density

				UO₂
2.117E+13	1.906E+13			UO₂/(Th-Pu)O₂ - Blanket
8.098E+12	7.070E+12			UO₂/(Th-Pu)O₂ - Ring
2.228E+13	1.976E+13			
5.893E+13	2.870E+13	2.912E+13	2.324E+13	
5.106E+13	1.260E+13	9.206E+12	5.820E+12	
6.449E+13	3.040E+13	2.835E+13	1.851E+13	
4.568E+13	6.730E+13	3.657E+13	2.979E+13	2.668E+13
4.697E+13	6.554E+13	3.024E+13	8.951E+12	7.423E+12
2.485E+13	3.898E+13	1.685E+13	1.045E+13	7.742E+12
6.883E+13	3.975E+13	6.471E+13	3.589E+13	4.586E+13
7.982E+13	4.480E+13	6.681E+13	3.167E+13	3.289E+13
8.019E+13	2.231E+13	3.454E+13	1.509E+13	1.044E+13
3.902E+13	6.491E+13	3.782E+13	6.298E+13	
5.038E+13	8.216E+13	4.483E+13	6.723E+13	
4.187E+13	6.778E+13	3.754E+13	6.108E+13	
6.379E+13	3.772E+13	6.396E+13		
8.952E+13	5.191E+13	8.343E+13		
5.884E+13	3.510E+13	6.092E+13		
3.772E+13	6.325E+13			
5.558E+13	9.171E+13			
3.204E+13	5.478E+13			
6.241E+13				
9.357E+13				
5.160E+13				

Fig. (6): Thermal Flux Distribution for 1/8 Core

Nuclear hot channel factors

It is important to note that replacing a third of AP1000 UO₂ fuel assemblies with (Th-Pu)O₂ fuel assemblies does not dramatically change the core's power distribution or induce hot channel factors beyond the prescribed limits. Local power density at the hottest part of a hot nuclear fuel rod should be estimated accurately to confirm that the rod does not melt.

The nuclear axial hot channel factor (F_Z^N) is defined as:

$$F_Z^N = \frac{Maximum\ heat\ flux\ of\ the\ hot\ channel}{Average\ heat\ flux\ of\ the\ hot\ channel}$$

- For UO₂, UO₂/(Th-Pu)O₂ blanket and UO₂/(Th-Pu)O₂ ring loading patterns, the axial hot channel factors of the core are 1.497 , 1.496 and 1.492, respectively

The nuclear radial hot channel factor (F_R^N) is defined as:

$$F_R^N = \frac{Average\ heat\ flux\ of\ the\ hot\ channel}{Average\ heat\ flux\ of\ the\ channels\ in\ the\ core}$$

- For UO_2, $UO_2/(Th\text{-}Pu)O_2$ blanket and $UO_2/(Th\text{-}Pu)O_2$ ring loading patterns, the radial hot channel factors of the core are 1.27 , 1.73 and 1.72, respectively.

The Total nuclear hot channel factor (power peaking factors) (F_q^N) is:

$$F_q^N = \frac{Maximum\ heat\ flux\ of\ the\ hot\ channel}{Average\ heat\ flux\ of\ the\ channels\ in\ the\ core}$$
$$= F_Z^N * F_R^N$$

- For UO_2, $UO_2/(Th\text{-}Pu)O_2$ blanket and $UO_2/(Th\text{-}Pu)O_2$ ring loading patterns, the hot channel factors of the core (power peaking factor) are 1.901, 2.588 and 2.566, respectively, which are under the design limit, 2.6.

Critical heat flux (CHF)

There are strict regulatory requirements concerning the flux and power distributions in power reactors. Likewise, to ensure that there is no risk of fuel melting, the fuel centerline temperature must be kept well within the melting temperature of the fuel. This requirement is met by ensuring that the critical heat flux is never reached. CHF describes a thermal limit where a phase change in the reactor coolant occurs during heating. The CHF occurs when the bubble density from nucleate boiling in the boundary layer of a fuel rod is so great that adjacent bubbles coalesce and form a vapor film on the surface of the rod. Heat transfer across the vapor film is relatively low compared to the liquid, and the occurrence of CHF is accompanied by a marked increase in the cladding surface temperature. Under such conditions, a rapid oxidation (or even melting) of the cladding can take place. The critical heat flux is reflected in the departure from nucleate boiling ratio (DNBR), defined as the ratio between the CHF (the heat flux is needed to cause departure from nucleate boiling) and the local heat flux of a fuel rod. The CHF summary is presented in Table (6) (W-3 correlation is used for CHF). The axial MDNBR of the hot channel is presented in Fig. (7). Over the length of the hot channel (4.166 m), the DNBR varies with a minimum of 2.887, 1.561 and 1.957, respectively, for UO_2, $UO_2/(Th\text{-}Pu)O_2$ blanket and $UO_2/(Th\text{-}Pu)O_2$ ring loading patterns, values are greater than those in the design limit, 1.3.

Each fuel assembly is defined as a channel region. The axial average fuel assembly temperature is shown in Fig. (8) and the axial average fuel temperature for the hottest fuel rod with the maximum enthalpy can be seen in Fig. (9). Maximum enthalpy take values equal to (0.233 MJ/kg - 55.784 cal/g), (0.296 MJ/kg - 70.703 cal/g), (0.264 MJ/kg - 63.007 cal/g) for UO_2, $UO_2/(Th\text{-}Pu)O_2$ blanket and $UO_2/(Th\text{-}Pu)O_2$ ring loading patterns, respectively.
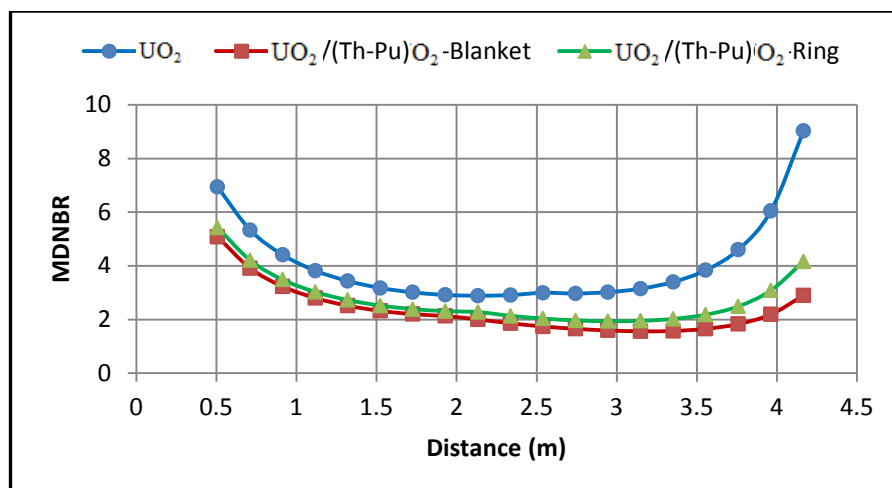
Fig.(7): Axial MDNBR of the Hot Channel

Table (6): Axial Critical Heat Flux Summary

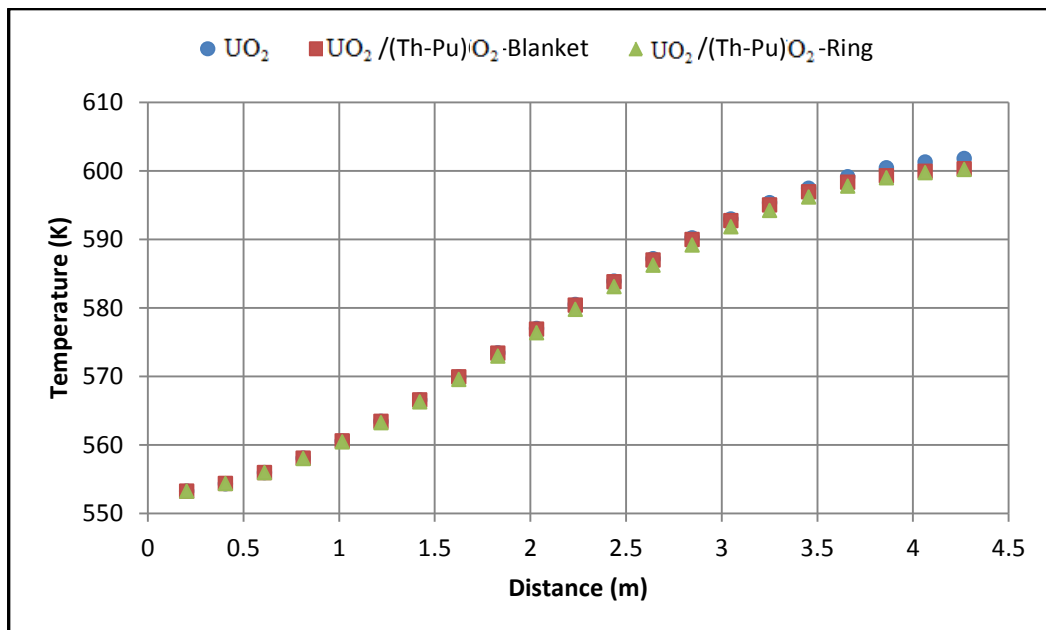| Distance (m)	Flux (MW/m²)			MDNBR		
	UO_2	UO_2/(Th-Pu)O_2 (Blanket)	UO_2/(Th-Pu)O_2 (Ring)	UO_2	UO_2/(Th-Pu)O_2 (Blanket)	UO_2/(Th-Pu)O_2 (Ring)
0.508	0.511	0.695	0.652	6.937	5.083	5.432
0.711	0.664	0.903	0.841	5.335	3.912	4.206
0.914	0.803	1.093	1.014	4.412	3.231	3.487
1.118	0.926	1.26	1.167	3.821	2.8	3.028
1.321	1.03	1.402	1.296	3.436	2.513	2.724
1.524	1.114	1.515	1.399	3.175	2.323	2.52
1.727	1.174	1.598	1.474	3.011	2.199	2.388
1.93	1.212	1.648	1.52	2.916	2.129	2.313
2.134	1.223	1.665	1.536	2.887	2.002	2.277
2.337	1.212	1.648	1.52	2.912	1.858	2.138
2.54	1.174	1.598	1.474	2.996	1.741	2.035
2.743	1.114	1.515	1.399	2.971	1.653	1.967
2.946	1.03	1.402	1.296	3.019	1.592	1.937
3.15	0.926	1.26	1.167	3.15	1.561	1.951
3.353	0.803	1.093	1.014	3.403	1.574	2.023
3.556	0.664	0.903	0.841	3.838	1.653	2.181
3.759	0.511	0.695	0.652	4.602	1.831	2.49
3.962	0.348	0.472	0.45	6.049	2.191	3.085
4.166	0.196	0.266	0.278	9.03	2.897	4.164

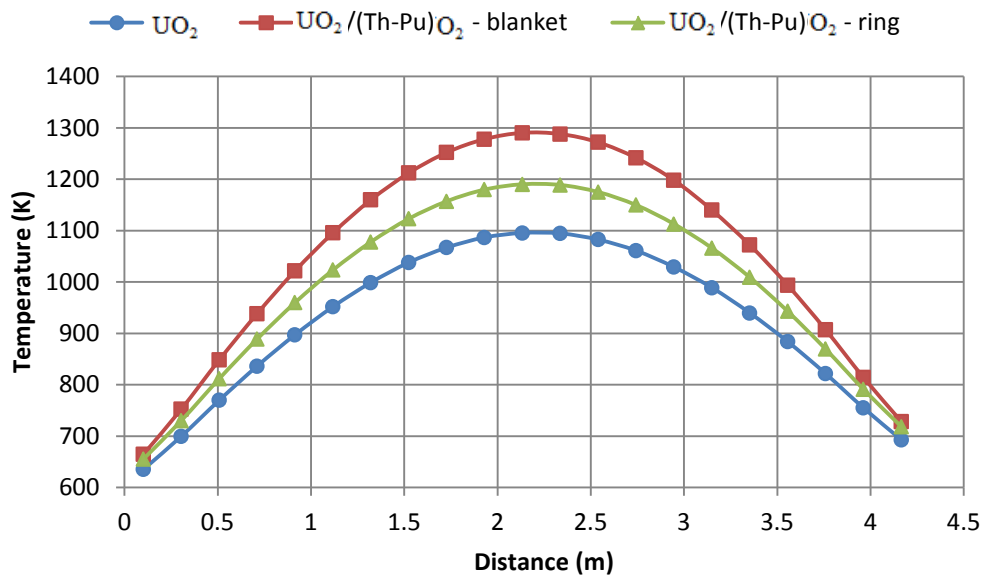**Fig.(8): Axial Average Fuel Assembly Temperature**

Fig.(9): Axial Average Temperature for Hot Fuel Rod

Conclusion

The results of the performed steady state analysis show that the two considered arrangements for (Th-Pu)O_2 fuel assemblies loading in the core (UO$_2$/(Th-Pu)O_2 blanket and UO$_2$/(Th-Pu)O_2 ring core loading schemes) can be used in AP1000, as the safety criteria mentioned in design control document are met.

The hot channel factors have a significant impact on the nuclear reactor safety margin and they affect the core thermal hydraulic design. These factors must remain below the design safety limits of the core during normal operation. In the present study, the power peaking factor was calculated for the considered UO$_2$/(Th-Pu)O_2 blanket and UO$_2$/(Th-Pu)O_2 ring loading patterns, the results indicate that the maximum value remains below the design limit, thus provides an adequate safety margin.

The Departure from Nucleate Boiling Ratio (DNBR) of the system is an important engineering design parameter for pressurized water reactors. The results of this study show that the calculated DNBR value for UO$_2$/(Th-Pu)O_2 blanket and UO$_2$/(Th-Pu)O_2 ring loading patterns is above the design limits.

This work provides the necessary basis for the study on Th-based fuel behavior and thermal hydraulic analysis of AP1000 using Th-based fuel to evaluate the safety aspect of various core loading patterns under anticipated and accidental conditions.

References

1- IAEA-TECDOC-1349, International Atomic Energy Agency Potential of thorium-based fuel cycles to constrain plutonium and reduce long lived waste toxicity (2003).

2- IAEA-TECDOC- 1450, International Atomic Energy Agency Thorium fuel cycle – Potential benefits and challenges (2005).

3- IAEA-TECDOC-1496, International Atomic Energy Agency Thermophysical properties database of materials for light water reactors and heavy water reactors (2006).

4- Klara Insulander Bjork Thorium-plutonium fuel for long operating cycles in PWRs - preliminary calculations, The Southern African Institute of Mining and Metallurgy, Thorium and Rare Earths(2012).

5- CheukWah Lau, Henrik Nylén, Klara Insulander Björk and Urban Sandberg Feasibility study of 1/3 thorium-plutonium mixed oxide core, Hindawi Publishing Corporation, Science and Technology of Nuclear Installations(2014).

6- A. Naymushin, YU. Chertkov, I. Lebedev, M. Anikin and S. Savanyuk Use of thorium in thermal-neutron reactors: different types of fuel compositions in VVER-1000 reactor cell, Jr. of Industrial Pollution Control(2016).

7- IAEA-TECDOC-1578, International Atomic Energy Authority Computational Analysis of the

Behavior of Nuclear Fuel under Steady State, Transient and Accident Conditions (2007).

8- Omid Noori-Kalkhoran, Abdolhamid Minuchehr, Amir Saied Shirani and M. Rahgoshay Full scope thermal-neutronic analysis of LOFA in a WWER-1000 reactor core by coupling PARCS v2.7 and COBRA-EN, Progress in Nuclear Energy, 74, pp. 193–200(2014).

9- Westinghouse European design control document, Rev.1 (2011).

10- Advanced reactors information system, status report 81 Advanced Passive PWR AP1000, International Atomic Energy Authority (2011).

11- QUARK, code system for 2-Group, 3D neutronic kinetics calculations coupled to core thermal hydraulic, RSICC (2000).

12- WIMS-D5, Winfrith Improved Multigroup Scheme Code System, RSICC (1991).